Acta Neuropathol (Berl) (1982) 58:1–8

Acta Neuropathologica

Original Works

Primary Demyelination in Experimental Canine Distemper Virus Induced Encephalomyelitis in Gnotobiotic Dogs

Sequential Immunologic and Morphologic Findings*

R. J. Higgins[1], S. G. Krakowka[2], A. E. Metzler[3], and A. Koestner[4]

[1] Institut für vergleichende Neurologie, Universität Bern, CH-3001 Bern, Switzerland
[2] Dept. of Veterinary Pathobiology, College of Veterinary Medicine, The Ohio State University, Columbus, OH 43210, USA
[3] Institut für Virologie, Universität Zürich, Winterthurerstr. 266A, CH-8057 Zürich, Switzerland
[4] Dept. of Pathology, Michigan State University, East Lansing, MI 48824, USA

Summary. Experimental infection of gnotobiotic Beagle dogs at 21 days of age with neurovirulent R252 strain of canine distemper virus (R252-CDV) resulted in a non-suppurative encephalomyelitis. Segmental internodal primary demyelination was found in almost 90% of the dogs from 27 days post inoculation (DPI). Ultrastructurally demyelination was initiated by the insertion of CDV-infected astrocytic processes at nodes of Ranvier with subsequent cleavage of well-preserved myelin from the axolemma. CDV-infected macrophages were consistently involved in myelin phagocytosis. Some remyelination of denuded axons occurred after 35 DPI. Persistent productive infection of the choroid plexus and ependyma in the fourth ventricle was consistently associated with subependymal foci of demyelination.

Primary demyelination occurred without detectable CDV-specific virus-neutralizing (CDV-VN) antibody in either serum or cerebrospinal fluid (CSF). There were no immunoglobulin deposits or inflammatory cells within the lesions. These findings indicate that both direct CDV antibody-dependent and CDV antibody-dependent cell-mediated immune mechanisms of cytolysis or myelin destruction are not involved in the genesis of initial primary demyelination. The sequential morphologic and serologic findings in this model of demyelinating encephalomyelitis indicate that direct virus-induced injury has a major role in both the initiation and early progression of primary demyelination.

Key words: Canine – Canine distemper virus – Demyelination – Encephalomyelitis – Antibodies

Introduction

Despite recent ultrastructural studies on natural [23, 32] and experimental [20, 26] CDV-induced demyelinating encephalomyelitis, the actual mechanism of primary demyelination remains controversial [23]. Some investigators favor direct virus-induced oligodendroglial or myelin injury [23] while others [10, 31] postulate primary humoral or cell-mediated immune mechanisms of demyelination. Recently, antibody and complement dependent [6], and lymphocyte-mediated anti-CDV directed cellular cytoxic immune mechanisms have been demonstrated in vitro [24]. Similar events could occur in vivo.

The age-dependent variation in both the immunologic and neuropathologic host response to CDV is well-known [13]. In our laboratory manipulation of the canine model for CDV-induced demyelinating encephalomyelitis by inoculation at 21 days of age rather than at 4–8 weeks [9] has resulted in a much higher incidence of consistent demyelinating lesions in the rostral medullary velum (RMV) (R. J. Higgins et al., unpublished data 1980). This finding has thus enhanced the potential usefulness of this model for sequential morphologic and immunologic studies designed to critically evaluate the temporal role of both viral and immune factors in vivo. The first objective of this study therefore was to examine the sequential histologic and ultrastructural morphogenesis of the earliest lesions leading to primary demyelination in the RMV and to correlate these changes with the presence of any viral antigen or immunoglobulin

* Supported by The State of Ohio Canine Research Fund and Grant Number 2 ROI NS 14821, National Institutes of Health, USA. A.E.M. was supported by the Schweizerische Stiftung für Medizinisch-biologische Stipendien, Basel and the Janggen-Pohen-Stiftung, St. Gallen, Switzerland

Offprint requests to: Dr. R. J. Higgins, 2300 Commonwealth Ave., Newton, MA 02166, USA

0001-6322/82/0058/0001/$1.60

deposits within these sites. The second aim was to interpret these findings in relation to parallel sequential studies to detect any CDV-associated humoral immune responses.

Material and Methods

Animals

A total of 20 gnotobiotic dogs from 6 litters were derived by caesarian section from date-mated CDV sero-negative pregnant Beagle bitches. They were raised in flexible plastic isolators using conventional techniques by methods described elsewhere [4, 14]. The animals were examined clinically twice daily.

Virus Inoculum

At 21 days of age, 17 dogs each received intraperitoneally 0.2 ml of freshly thawed 20% spleen-thymus homogenate, containing $10^{4.5}$ canine pulmonary macrophage culture infective doses of neurovirulent R252-CDV per ml ($PMCID_{50}$/ml). The origin and in vivo properties [20, 21] of this virus have been reported. Three dogs were maintained separately in isolators as uninoculated controls. At intervals of 8, 10, 14, 18, 21, 24, 27, 31, 35 and 42 DPI dogs were killed with 2, 1, 1, 2, 2, 1, 4, 1, 1 and 2 dogs on each day, respectively. Uninoculated controls dogs were killed at 28, 43 and 70 days of age.

Virologic and Immunologic Studies

Both clotted and unclotted blood samples were collected once prior to inoculation and at weekly intervals from control and CDV-infected dogs and evaluated for total and differential white blood cell counts. In addition, an aliquot from each was evaluated for leukocyte-associated viremia using a direct immunofluorescence technique as described previously [13]. Dextran-saline sedimented peripheral blood lymphocytes were tested for in vitro lymphocyte blast transformation (LBT) using plant mitogens phytohemaglutinin-P and pokeweed [11]. Cell-free preparations of cerebrospinal fluid (CSF) were assayed from 2 dogs for infectious CDV using canine pulmonary macrophage cultures [12]. Cells recovered from the CSF samples from 12 dogs without clinical signs were evaluated for the presence of viral antigen by direct immunofluorescence. Serum and CSF antibody titers to R252-CDV were determined using a microtiter virus neutralisation (VN) system [2].

Histopathology and Immunofluorescence (IF)

Under deep anesthesia, a CSF sample was taken from the cisterna magna, the left half of the brain of the 20 dogs was removed aseptically, followed by perfusion fixation of each dog for subsequent morphologic examination. Six selected blocks of fresh CNS tissue from all the CDV-infected dogs and the 3 uninoculated dogs were processed by routine techniques for direct IF [27]. These included direct IF staining for both CDV antigens and immunoglobulins, using fluorescein-isothiocyanate-labelled rabbit anti-CDV immunoglobulin G and rabbit anti-dog polyvalent immunoglobulin (Miles Research Labs., Inc.) respectively. Sites routinely examined for the presence of virus and immunoglobulins were the olfactory bulb and tract, frontal and temporal cortex, basal ganglia, hippocampus, thalamus, midbrain, cerebellar cortex, choroid plexus of the fourth ventricle, cerebellar peduncles and medulla oblongata. Similarly processed tonsilar or lymph node tissue from conventionally raised dogs was used as positive control material for immunoglobulin staining. After IF examination some CNS sections were counterstained with Giemsa for correlation between presence of virus and histologic lesions.

Sixteen half-coronal sections from the remaining half perfused brain of each dog were processed by routine techniques for light microscopy, stained with hematoxylin-eosin (H-E) and selected sections also with luxol fast blue-cresyl echt violet (LFB-CEV). The intact RMV was carefully removed, post fixed and selected pieces immediately processed routinely for electron microscopy [19]. Sections 1 µm thick cut from the longitudinally or transversely oriented blocks were stained with alkaline toluidine blue and then examined by light microscopy. Thin sections were cut from selected sites of the relevant blocks, mounted and stained with uranyl acetate and then lead citrate before ultrastructural examination.

Results

Hematology, Virology and Immunology

From 7 DPI, all infected dogs had a sustained leukopenia mainly due to a relative or absolute lymphopenia. There was a cell-associated viremia as determined by IF in all dogs to 21 DPI. Four of the dogs were IF positive at 28 DPI and 1 dog was viremic throughout the course of infection. Free infectious virus was not detected in the CSF from two dogs examined terminally at 31 and 42 DPI. However, CDV antigen was consistently demonstrated in cells recovered from the CSF in all the 12 inoculated dogs which were tested. One dog had a terminal serum CDV-VN antibody titer of 1:16 when killed 27 DPI, but previous weekly samples from this dog and serum and CSF samples from all the other dogs tested had no antiviral antibodies (see Table 1). Phytomitogen-induced LBT assays for both T- and B-cell-responsive lymphocyte populations remained consistently depressed compared to the controls throughout the course of infection [16].

Clinical Findings

No clinical neurologic signs were observed in 13 dogs killed between 8 and 42 DPI. In the remaining four dogs the earliest common clinical signs, starting between 24 and 31 DPI, were depression, anorexia and occasional respiratory distress followed within 12–24 h by isolated irregular myoclonus of facial or limb muscles, mild truncal ataxia and intermittent, unintentional fine head tremors. Intermittent facial myoclonus with salivation progressed within 24–72 h to grand-mal seizures of increasing intensity with decreasing intervals between their onset. Dogs became prostrate once continuous seizures developed and were then killed. One dog had no other premonitory clinical signs prior to the sudden onset of grand-mal convulsions. Rectal temperatures of all dogs remained within normal levels (38.3–38.5° C) throughout the course of infection with elevation to 40.1° C only in dogs at terminus.

Immunofluorescent Findings

Earliest detectable CDV-IF antigen was restricted to the cytoplasm of isolated mononuclear cells randomly

Table 1. Significant sequential clinical, morphologic and immunologic data from CDV-infected gnotobiotic dogs

	Days post inoculation (DPI)									
	8	10	14	18	21	24	27	31	35	42
No. of dogs in group	2	1	1	2	2	1	4	1	1	2
Dogs with neurologic signs[a]	neg	neg	neg	neg	neg	1	(2)	1	neg	(1)
Light microscopic lesions[b]	neg	neg	neg	neg	neg	AB	ABC	ABC	AB	ABC
Ischaemic neuronal necrosis	neg	neg	neg	neg	neg	+	(2)+	+	neg	(1)+
Demyelination in RMV	neg	neg	neg	neg	neg	neg	+	+	neg	+
VN antibody titres CSF	neg	neg	neg	neg	neg	neg	neg	neg	neg	neg
VN antibody titres Serum[c]	neg	neg	neg	neg	neg	neg	1:16	neg	neg	neg
Immunoglobulin in lesions	neg	neg	neg	neg	neg	neg	neg	neg	neg	neg
CDV antigen in lesions	neg	neg	neg	neg	neg	+	+	+	+	+

[a] Numbers in parenthesis indicate no. affected in group
[b] *A* Non suppurative meningitis, focal microgliosis
B Astrocytic hypertrophy, microglial cells
C Spongy vacuolation and loss myelin staining
[c] CDV-VN antibody titre expressed as serum dilution
\+ Positive
neg Negative

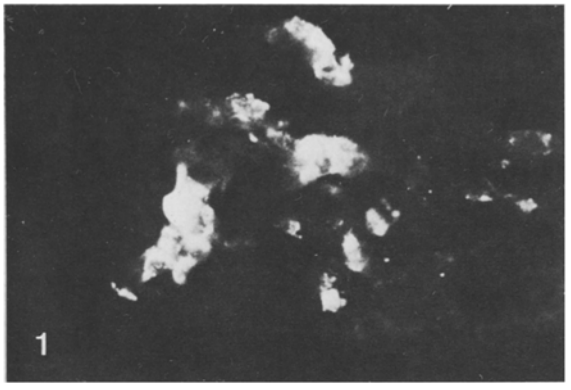

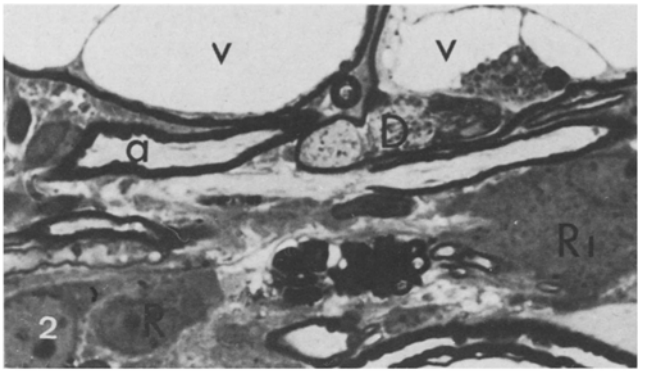

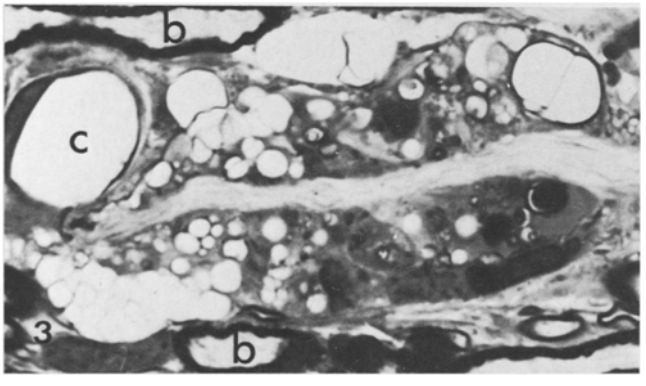

Fig. 1. Immunofluorescent photomicrograph of the choroid plexus of the fourth ventricle with multiple foci of IF-positive viral antigen in epithelial cells. 18 DPI, × 450

Fig. 2. A segmentally demyelinated, structurally intact axon with intact myelin sheath at adjacent internode. Naked axon adjacent to intact myelinated axon (*a*). Degenerating axon (*D*) also with intact myelin. Reactive astrocytes (R_1, *R*) with one (R_1) adjacent to intact myelin. Intra-axonal vacuoles (*V*). In RMV. 27 PDI, × 600

Fig. 3. A longitudinal profile of a demyelinated intact axon surrounded by two infected macrophages containing myelin and granular debris and vacuoles. Note intact adjacent myelinated axons (*b*) and dilated capillary (*C*) without perivascular cellular infiltrate. In RMV. 27 DPI, × 600

distributed in the meninges of the spinal cord and brain at 10 DPI.

By 14 DPI, antigen was detected in single isolated neurons within the grey matter of the frontal, temporal and cerebellar cortex together with occasional fluorescence within the parenchyma adjacent to blood vessels in grey matter. Single infected ependymal cells were found in the ependymal lining of lateral, third and fourth ventricles and in the choroid plexus epithelium of the fourth ventricle. At 18 DPI, multiple clusters of infected epithelial cells were seen in the choroid plexus and ependyma of the fourth ventricle (Fig. 1). Within the CNS parenchyma, IF positive single neurons contained granular or diffuse cytoplasmic fluorescence and sometimes intranuclear inclusions. From the perikaryon there was extension of

the fluorescence into thin slender filamentous processes. The distribution though widespread, was restricted to single cells in the grey matter, although occasional fluorescent cells presumably astrocytes, were noted in the white matter of the cerebellar folia. There was no suggestion of centripetal viral spread from the olfactory bulbs. Infected ependymal cells were demonstrated in the central canal of the spinal cord. Between 24 and 31 DPI the pattern of distribution did not change. Infected neurons occurred in clusters. Increased numbers of virus antigen-containing cells were demonstrated within the meninges.

Blood vessels in the grey, and less often in the white matter, had prominent perivascular foci of antigen restricted to cells in the parenchyma. There was no perivascular mononuclear cell cuffing at any time. Foci of infected granule cells in the cerebellar folia were not always associated with necrosis. By Giemsa counterstaining two areas of intense sub-pial fluorescence in the midbrain and medulla oblongata histologically had edema, demyelination and hypertrophic astrocytes. Throughout the course of this study, immunoglobulin deposits as determined by IF were not detected within the CNS including even those sites with microscopically visible lesions (Table 1).

Light Microscopy

Coronal Sections of the CNS. Of the 13 dogs without neurologic signs killed between 8 and 42 DPI, only the five dogs killed beginning at 24 DPI had microscopic CNS lesions. These consisted of non-suppurative meningitis, widespread mild multifocal microgliosis, and neuronal degeneration with or without neurophagia confined mainly to the grey matter of the cerebral cortex, hippocampus, medulla oblongata and spinal cord. The most intense microgliosis occurred in the frontal and temporal cortex. Both intranuclear and intracytoplasmic eosinophilic inclusion bodies were found within morphologically intact neurons particularly within the cerebral cortex and in the midbrain.

By 24 DPI small multifocal subpial or subependymal foci of increased cellularity, including hypertrophic astrocytes, were consistently found around the fourth ventricle in the medulla oblongata and in the pons and spinal cord. In these areas from 27 to 31 DPI other alterations consisted of vacuolar spongy change with loss of myelin staining as demonstrated by LFB-CEV staining. There were also microglial and active gitter cell accumulations. By 35 DPI additionally there was some confluent malacia. Between 35 and 42 DPI, three dogs also had concurrent multifocal malacia with cyst formation and similar associated cell types in foci of the parietal and frontal cerebral cortex. Perivascular cuffing was not found in any of these lesions. One dog killed at 27 DPI with a terminal serum VN antibody titer of 1:16 and negative CSF titre had widespread unique individual axonal necrosis with demyelination in cerebral white matter of the frontal, parietal and occipital lobes. No lesions were found in the overlying grey matter.

One dog without observed neurologic signs killed at 42 DPI had striking acute ischaemic neuronal necrosis without associated inflammatory cell response. These multifocal, bilateral and symmetrical lesions were found mainly in the temporal cortex, including the amygdala and hippocampus. In the four dogs killed after sustained terminal seizures there were varying degrees of similarly distributed bilaterally symmetrical ischaemic neuronal necrosis (Table 1).

Rostral Medullary Velum. Lesions in the RMV were similar in temporal sequence and severity to those demyelinating lesions in the other sites in the CNS. The earliest lesion was an increased number of reactive astrocytes, either singly or in clusters, randomly distributed between intact myelinated axons at 24 DPI. Some astrocytes were bi- or multinucleate. Many astrocytes had single intranuclear or multiple intracytoplasmic CDV inclusion bodies. Single myelinated axons had sharply demarcated segments of the axolemma devoid of myelin adjacent to normally myelinated internodes (Fig. 2). Many individual demyelinated axons were found in areas without cell infiltration and often abutted normal myelinated axons. Conversely, the cytoplasmic membrane of many infected reactive astrocytes bordered intact myelinated internodes of demyelinated axons. Adjacent blood vessels were normal (Fig. 2).

By 27 DPI other partially or completely demyelinated axons were surrounded by actively phagocytic cells containing CDV neucleocapsids, myelin and granular debris and multiple empty vesicles (Fig. 3). The axons undergoing active demyelination were surrounded by intact parenchyma and normal blood vessels. Occasionally structurally intact axons had segments of myelin sheath thinning or vacuolation without phagocytosis.

Although many CDV-infective reactive astrocytes were found between intact myelinated axons some were adjacent to demyelinated axon segments. These cells had no evidence of active myelin phagocytosis before 35 DPI. No changes were detected in oligodendroglia in these areas although precise morphologic identification of all cells could not be made. Focal loss or attenuation of overlying ependymal epithelium was common.

By 42 DPI there was almost total demyelination of all axons which lay within a network of astrocytic

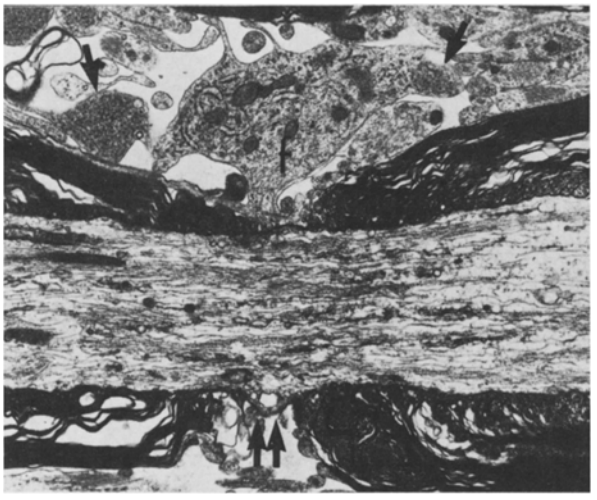

Fig. 4. A structurally intact myelinated axon with multiple cytoplasmic processes containing nucleocapsids (*arrows*) and glial filaments (*f*) adjacent to the axolemma at the node of Ranvier. Normal exposed axolemma (*double arrows*). 24 DPI, ×6,000

processes. These processes surrounded many of the intact naked axons in the loose edematous matrix. Numerous phagocytic cells were distended with myelin debris.

Blood vessels were prominent but had no perivascular inflammatory cell cuffing. Swollen degenerating axons had either partially intact or vacuolar ballooning of myelin sheaths. Similar lesions were consistently found in sub-ependymal sites of the medulla close to the origin of the RMV.

Ultrastructural Lesions

Rostral Medullary Vellum. The earliest ultrastructural change in morphologically intact myelinated axons was the insertion of nucleocapsid-bearing astrocytic cell processes onto nodes of Ranvier between intact paranodal areas and their subsequent attachment to the exposed axolemma at 24 DPI (Fig. 4). This attachment zone did not always completely encircle the node. At 27 DPI in segmentally demyelinated axons, these cell processes initially inserted under the myelin paranodal-axonal junction and then extended between the axolemmae and overlying myelin lamellae, with relative preservation of the separated myelin sheath. Vacuolar intramyelinic lamellar separation did not occur around axons undergoing cell-mediated segmental internodal stripping of the myelin sheath. Tight junctions between astrocytic cell processes were often found. Also by 27 DPI nucleocapsid-containing actively phagocytic cells surrounded many demyelinated but intact axons. Their elongate nuclei often had multiple indentations and uniformly dispersed abundant heterochromatin. The dense, dark staining cytoplasm contained abundant rough endoplasmic reticulum, multiple clusters of lamellar myelin-like profiles, lipid inclusions, granular debris and prominent lysosomes but no filaments or microtubules. These cells surrounded single intact denuded axonal segments while neighboring adjacent myelinated axons were intact. Sometimes these cells were between other naked axons (Fig. 5). Although infected hypertrophic astrocytes containing glial filaments were adjacent to myelinated or demyelinated axons, these cells did not have evidence of phagocytosis of myelin before 35 DPI. By 35 DPI some axons had thin attenuated myelin sheaths of uniform thickness but with intact paranodal junctions suggesting remyelination (Fig. 7). Other axons had multiple compacted myelin-like lamellae membranes. By 42 DPI cytoplasmic processes of reactive CDV-containing astrocytes were often found wrapped around groups of naked axons (Fig. 6).

Choroid Plexus. Between 18 and 42 DPI, nucleocapsid containing choroid plexus and ependymal epithelium of the fourth ventricle had parallel dense intramembranous spikes along the luminal cytoplasmic border. Budding to form mature intact virions occurred along most of the plasmalemma between existing microvilli and cilia (Fig. 8). Although some mononuclear cells in the meninges did have similar membrane spiking, viral budding suggestive of productive viral replication was not seen in these or any other CNS cells.

Discussion

This study demonstrated that experimental infection with neurovirulent R252-CDV in gnotobiotic dogs at 21 days of age resulted in a non-suppurative encephalomyelitis with primary demyelination occurring in almost 90% of the dogs from 27 DPI. Compared to other experimental studies [1, 20] this high incidence of primary demyelination in the RMV in our dogs thus significantly enhances the potential usefulness of this model [9] for the investigation of proposed mechanisms of CDV-induced demyelinating encephalomyelitis in vivo. Initial segmental internodal demyelination was always associated with CDV in the lesions but occurred without either detectable CDV-VN specific antibody response in the serum or CSF, perivascular mononuclear cell cuffing or immunoglobulin deposits within lesions.

In the known predilection sites of CDV induced primary demyelination, the earliest change was increased numbers of hypertrophic CDV-infected astrocytes. Ultrastructurally, astrocytic cell processes containing glial filaments and nucleocapsid were closely applied to the axolemma at the nodes of Ranvier. Subsequent disruption of paranodal junctions of relatively intact myelin by these underrunning processes

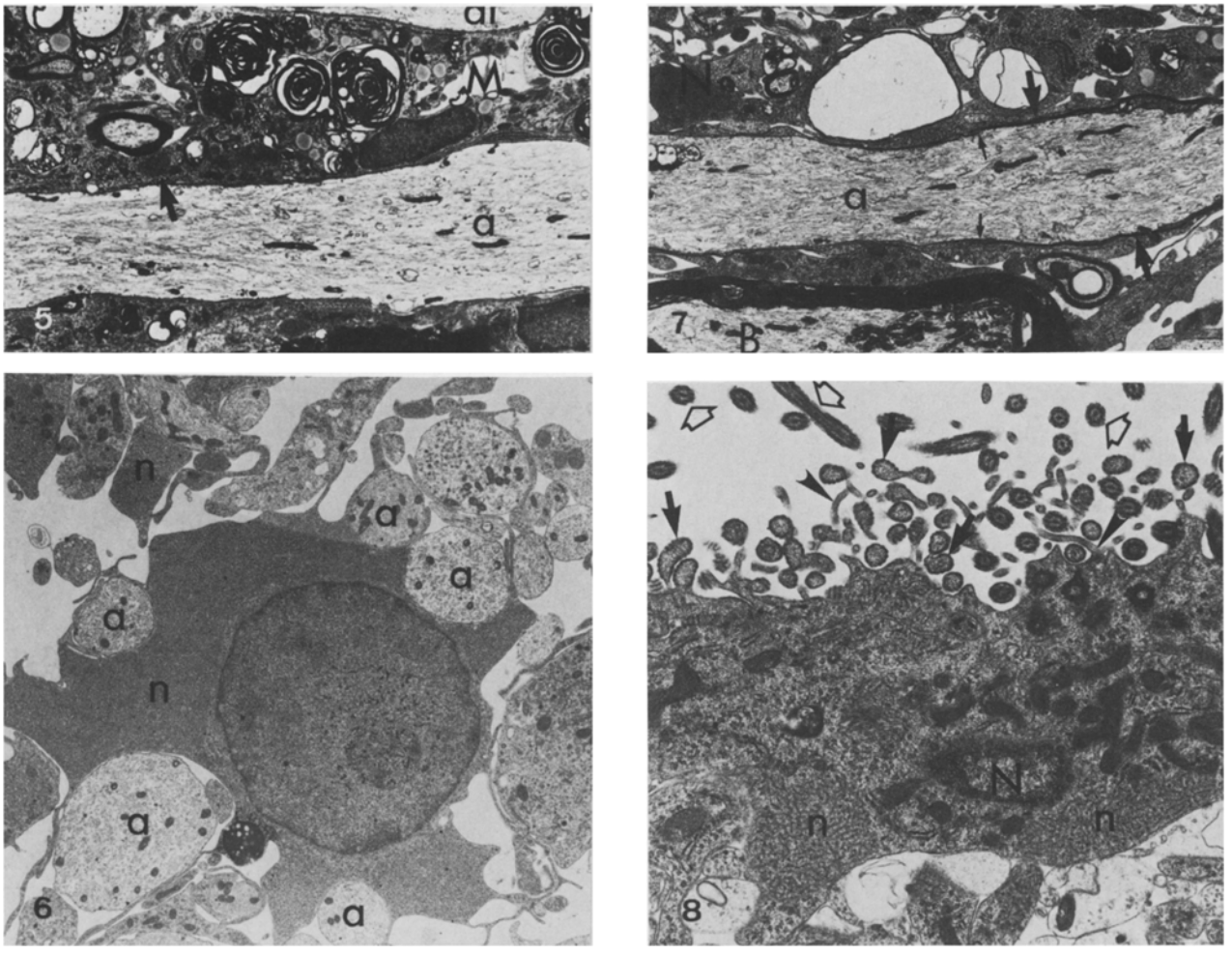

Fig. 5. Between two demyelinated axons (*al*, *a*) a phagocytic cell (*M*) containing nucleocapsids (*arrow*) and myelin-like debris, lipid, abundant RER and lysosomes but no glial filaments. 31 DPI, ×3,000

Fig. 6. Reactive astrocyte containing nucleocapsid (*n*) aggregates with cell processes extending around demyelinated intact axons (*a*). 42 DPI, ×2,000

Fig. 7. Thinly remyelinated axon (*a*) with intact paranodal attachments (*small arrows*). Loosely compacted myelin-like lamellar membrane partially covering the remainder of the axon (*arrows*). Nucleocapsid (*N*). Note normal thickness of myelin around axon (*B*). 35 DPI, ×3,000

Fig. 8. On the floor of the fourth ventricle, ependymal cell with nucleus (*N*). Multiple intracytoplasmic nucleocapsid aggregates (*n*) cytoplasmic border with virus-specific electron-dense spikes, numerous budding or mature virions (*arrows*); intact cilia (*open arrows*) and microvilli (*arrowheads*). 31 DPI, ×7,000

suggests a primary role for infected astrocytes in the initial demyelinating processes. Although these early changes have not been reported, phagocytosis of myelin lamellae by astrocytes in CDV-induced demyelination has been recognised previously in both spontaneous [23] and experimental studies [26]. In our series myelin phagocytosis was mediated by CDV-infected macrophages several days before similar participation by astrocytes.

Although a scavenger role for CDV-infected macrophages around denuded axons [26] has been confirmed in this study, their role in initiating primary demyelination remains speculative. The highly selective pattern of internodal myelin destruction appears incompatible with that from extracellular release of myelinolytic proteases from CDV-infected macrophages, as demonstrated in vitro with non-specifically activated macrophages [3]. Our morphologic interpretation however would be consistent with a mechanism of intracellular protease-induced myelinolysis following CDV-induced macrophage fusion with individual oligodendroglia or their membranes. In our

study, such a non-specific bystander mechanism of myelin injury would not be dependent on any antiviral humoral response [31]. Unequivocal identification of these phagocytic cells could be best resolved by the application of specific cell marker labelling techniques [8].

The segmental internodal uniform myelin loss over denuded axons, sharply demarcated from adjacent intact myelin parnodal attachments, suggests a primary and highly selective insult to oligodendroglia or their myelin lamellae. Although CDV infection of oligodendroglia is rare [23, 27] and was not recognized in this study, a non-cytolytic infection of these cells could result in this pattern of demyelination. This pattern is similar to that of experimental coronavirus-induced demyelinating encephalomyelitis in mice where virus-induced cytolysis of oligodendroglia results in primary segmental demyelination [29]. It contrasts sharply with the multifocal, irregular lysis of myelin lamellae and primary demyelination with perivenular mononuclear cell infiltrates characteristic [18] of experimentally-induced autoimmune-mediated acute [17] and chronic [25] experimental allergic encephalitis. The finding in our dogs of inappropriately thin internodal myelin sheaths of uniform thickness that terminated in normal paranodal complexes fulfill the established criteria for remyelination within the CNS [22]. Thus, the presence of remyelination after 35 DPI implies a capacity for functional restoration of injured oligodendroglia or remyelination from other intact oligodendroglia as in corona virus infection in mice where remyelination occurs as early as 24–28 DPI [30].

Because CDV replicates by surface budding following incorporation of viral glycoproteins in cell surface membranes, CDV-infected cells expressing surface membrane antigens are excellent targets for CDV-antibody dependent cytolysis as demonstrated in vitro [6, 24]. CDV nucleocapsids were demonstrated in neurons and glial cells in demyelinating lesions, but only infected mononuclear cells in meninges and choroid plexus and the ependymal epithelium had characteristic membrane spiking. This data, with the absence of CDV antibody in serum or CSF and lack of detectable immunoglobulin deposits or immunocompetent cells in the lesions, indicates that it is highly unlikely CDV-VN antibody-dependent mechanisms are involved in initial primary demyelination.

Apparent exacerbation of histologic lesions in the cerebral cortex of neonatal CDV-infected gnotobiotic dogs has been achieved by the administration of specific CDV-VN antibody during the course of infection [15]. In the one dog with terminally detected serum CDV antibody activity, a similar antibody-induced modulation may explain the additional unique demyelinating lesions in the cerebral hemispheric white matter. However, in this dog there was no discernable difference in the severity and focal nature of the demyelinating lesions in other sites compared with those of the three seronegative dogs. This observation suggests again that humoral immune mediated mechanisms play little or no part in the initiation of demyelination.

In five dogs bilateral and symmetrically distributed ischaemic neuronal necrosis was found in the predilection sites of the paleocortex, essentially similar to that occurring in spontaneous CDV-associated polioencephalomalacia [28]. Although seizure activity with induced hypoxia has been postulated to account for these lesion [28] similar histologic lesions were found in one dog without observed neurologic signs. The lesions may in fact result from direct neuronal infection with CDV. Widespread CDV-associated neuronal necrosis in experimental infection in gnotobiotic dogs has recently been described [5]. From the IF findings virus antigen spread within the CNS occurred via the vascular route and not centripetally within the rhinencephalon as has been suggested to account for this lesion distribution [28].

The demonstration of a productive infection of the choroid plexus and ependymal epithelium throughout the course of infection in the CDV-seronegative dogs was essentially similar to that found in a previous study of CDV-infected neonatal dogs [5]. The occurrence in this study of classical demyelination in both subependymal and sub-pial sites [7] suggests that the proximate source of free virus within the CSF maybe a factor in the initiation of these topographically restricted lesions.

In conclusion, the high incidence of demyelination in the RMV and the lack of a detectable CDV-specific humoral response, features of infection at 21 days of age, allowed a critical in vivo evaluation of certain postulated humoral immune-mediated mechanisms of demyelination. Direct CDV-induced injury appears to play a major role in initiation of the primary demyelination. The absence of specific CDV antibody in these dogs with multifocal demyelinating lesions suggests that the genesis of initial primary demyelination in CDV-induced encephalomyelitis at this age occurs independently of both direct and indirect humoral antiviral immune mechanisms.

Acknowledgements. The authors wish to acknowledge the excellent technical assistance of David Long, Nancy J. Austin, Addajane Wallace and Sue Ringler.

References

1. Appel MJG, Gillespie JH (1972) Canine distemper virus. Virol Monogr 10:1–96
2. Appel MJG, Robson DS (1973) A micro-neutralization test for canine distemper virus. Am J Vet Res 34:1459–1463

3. Cammer W, Bloom BR, Norton WT, Gordon S (1978) Degradation of basic protein in myelin by neutral proteases secreted by stimulated macrophages: A possible mechanism of inflammatory demyelination. Proc Natl Acad Sci USA 75:1554–1558
4. Greisemer RG (1963) The gnotobiotic dog. Lab Anim Care 13:643–649
5. Higgins RJ, Krakowka S, Metzler AE, Koestner A (1982) Experimental canine distemper encephalomyelitis in neonatal gnotobiotic dogs – a sequential ultrastructural study. Acta Neuropathol (Berl) 57:287–295
6. Ho CK, Babiuk LA (1980) Immune mechanisms against canine distemper. Immunology 39:231–237
7. Innes JRM, Saunders LZ (1962) Comparative neuropathology. Academic Press, New York, pp 373–384
8. Kennedy PGE, Lisak RP, Raff MC (1980) Cell type-specific markers for human glial and neuronal cells in culture. Lab Invest 43:342–351
9. Koestner A (1975) Animal model – distemper-associated demyelinating encephalomyelitis. Am J Pathol 78:361–364
10. Koestner A, McCullough B, Krakowka S, Long JF, Olsen RG (1974) Canine distemper: A virus-induced demyelinating encephalomyelitis. In: Zeman W, Lenette (eds) Slow virus diseases. Williams & Wilkins, Baltimore, pp 86–101
11. Krakowka S, Cockerell G, Koestner A (1975) Effects of canine distemper virus infection on lymphoid function in vitro and in vivo. Infect Immun 11:1069–1078
12. Krakowka S, Higgins RJ, Metzler AE (1980) Plasma phase viremia in canine distemper virus in gnotobiotic dogs. J Infect Dis 134:629–632
13. Krakowka S, Koestner A (1976) Age-related susceptibility to infection with canine distemper virus in gnotobiotic dogs. J Infect Dis 134:629–632
14. Krakowka S, Long D, Mezza R, Mador R, Koestner A (1978) Derivation and maintenance of gnotobiotic dogs. Lab Anim Sci 28:327–330
15. Krakowka S, Mador RA, Koestner A (1978) Canine distemper virus-associated encephalitis: Modification by passive antibody administration. Acta Neuropathol (Berl) 43:235–241
16. Krakowka S, Higgins RJ, Koestner A (1980) Canine distemper virus: Review of structural and functional modulations in lymphoid tissues. Am J Vet Res 41:284–292
17. Lampert PW (1965) Demyelination and remyelination in experimental allergic encephalomyelitis: further electron microscopic observations. J Neuropathol Exp Neurol 24:371–380
18. Lampert PW (1978) Autoimmune and virus-induced demyelinating diseases. Am J Pathol 91:176–197
19. Mador R, Krakowka S, Koestner A (1974) A procedure for processing central nervous system tissue for immunofluorescence, light and electron microscopic evaluation. Am J Vet Res 38:1946–1949
20. McCullough B, Krakowka A, Koestner A (1974) Experimental canine distemper virus-induced demyelination. Lab Invest 31: 216–222
21. McCullough B, Krakowka S, Koestner A, Shadduck J (1974) Demyelinating activity of distemper virus isolates in gnotobiotic dogs. J Infect Dis 130:343–350
22. Prineas JW, Connell F (1979) Remyelination in multiple sclerosis. Ann Neurol 5:22–31
23. Raine CS (1976) On the development of CNS lesions in natural canine distemper encephalomyelitis. J Neurol Sci 30:13–28
24. Shek WR, Schultz RD, Appel MJG (1980) Natural and immune cytolysis of canine distemper virus-infected target cells. Infect Immun 28:724–734
25. Snyder DH, Valsamis MP, Stone SH, Raines CS (1975) Progressive demyelination and reparative phenomena in chronic experimental allergic encephalomyelitis. J Neuropathol Exp Neurol 34:209–215
26. Summers BA, Greisen HA, Appel MJG (1979) Early events in canine distemper demyelinating encephalomyelitis. Acta Neuropathol (Berl) 46:1–10
27. Vandevelde M, Kristensen B (1977) Observations on the distribution of canine distemper virus in the central nervous system of dogs with demyelinating encephalomyelitis. Acta Neuropathol (Berl) 40:233–236
28. Lisiak JA, Vandevelde M (1979) Polioencephalomalacia associated with canine distemper virus infection. Vet Pathol 16: 650–660
29. Weiner LP (1973) Pathogenesis of demyelination induced by a mouse hepatitis virus (JHM virus). Arch Neurol 28:298–303
30. Weiner LP, Stohlman SA (1978) Viral models of demyelination. Neurology 28:111–114
31. Wisniewski HM (1977) Immunopathology of demyelination in autoimmune diseases and virus infections. Br Med Bull 33: 54–59
32. Wisniewski HM, Raine CS, Kay WJ (1972) Observations on viral demyelinating encephalomyelitis: Canine distemper. Lab Invest 26:589–599

Received February 23, 1982/Accepted May 25, 1982